We are IntechOpen,
the world's leading publisher of
Open Access books
Built by scientists, for scientists

6,900
Open access books available

185,000
International authors and editors

200M
Downloads

154
Countries delivered to

Our authors are among the

TOP 1%
most cited scientists

12.2%
Contributors from top 500 universities

CLARIVATE ANALYTICS
BOOK CITATION INDEX
INDEXED

WEB OF SCIENCE™

Selection of our books indexed in the Book Citation Index
in Web of Science™ Core Collection (BKCI)

Interested in publishing with us?
Contact book.department@intechopen.com

Chapter

Fabrication of Fine-Grained Functional Ceramics by Two-Step Sintering or Spark Plasma Sintering (SPS)

Wallace R. Matizamhuka

Abstract

The majority of functional materials today are based on ceramic materials which find use in a wide range of applications that include magnetic, electronic, optical, thermoelectric (TE) and piezoelectric energy. The properties and reliability of functional ceramic materials are highly depended on the density, grain size and existence of heterogeneities in the microstructure. It is a well-known fact that there is property enhancement at finer grain sizes for most functional materials through a multitude of mechanisms depending on the application. However, what remains a challenge is the success in maintaining fine-grained microstructures using conventional sintering methods. The use of such methods results in uncontrollable grain growth and coarse microstructures which negate the benefits of fine-grained related properties. The use of spark plasma sintering (SPS) technique offers an opportunity to produce fine-grained microstructures with minimum grain growth. However, grain refinement is not always guaranteed during SPS sintering especially under high-temperature sintering conditions. Therefore, sintering conditions that allow densification with minimal grain growth are well suited for microstructural refinement. A modified two-step sintering (TSS) methodology in SPS has proven to yield promising results and has potential use in the production of functional ceramic materials with controlled microstructures.

Keywords: two-step sintering, functional ceramics, spark plasma sintering, functional properties, grain refinement

1. Introduction

Over the past few decades, functional ceramics have played a significant role in advanced technologies owing to their unique thermal, electrical, magnetic, opto-electrical, superconducting and gas-sensing properties. As such, functional ceramics have become the frontiers for advanced technologies such as information technology, medical technology, energy transformation, storage, supply and manufacture technology. For instance, functional ceramics are widely used for electronic applications as they can operate at high power and high frequencies, at high temperatures and harsh conditions. Their capability to combine properties such as electrical insulation and magnetism, which is not possible with metals, gives them an additive advantage.

Functional ceramics are produced from chemically synthesised powders in the form of oxides, nitrides, carbides and borides mainly through a powder metallurgy route. The properties of functional ceramics are microstructure sensitive, and microstructural features such as grain size, composition, homogeneity and grain boundary constituents are critical to their performance and reliability. The processing route dictates the final microstructural features obtained; thus, the choice/design of a processing route is key in material functionality. For instance, fine grain size has been experimentally proven to amplify functional material properties such as electrical conductivity, thermal conductivity, piezoelectric and ferroelectric properties [1]. It must be mentioned though that the fabrication of dense nanostructured functional ceramics by conventional sintering methods is quite challenging owing to the uncontrollable high grain growth rates [2]. This explains the shift in research focus towards nanostructured functional materials in the past few years.

In recent years, spark plasma sintering (SPS) technology has proven its capability to fabricate fine-grained microstructures possessing superior properties for a wide range of materials [2]. This method is increasingly being applied in the production of functional ceramic materials. It is against this background that the present chapter is aimed at giving an insight on the progress made so far and, furthermore, how the resulting microstructures and properties align with the required functions. It is imperative that a background on the various applications of functional ceramics be given prior to a detailed discussion on the SPS sintering methodologies.

2. The most popular functional ceramics and their applications

Functional ceramics are materials tailored to possess exceptional properties (electrical, thermal, optical, piezoelectric and magnetic properties) by controlling the composition and microstructures [3]. These materials are being utilised in a broad range of applications owing to the distinct advantages they offer in comparison to metals. The list below is not meant to be exhaustive but to give a qualitative review on the applications of the most popular functional ceramic materials.

2.1 Piezoceramics

Piezoelectric ceramic materials couple electrical and mechanical responses in their functioning and are widely used for electromechanical sensors and actuators. These materials normally produce an electrical response in the form of either a voltage or charge proportional to the applied stress when subjected to a mechanical force. Conversely, an applied voltage can be converted into mechanical energy such as in piezoelectric motors and sound-/ultrasound-generating devices. Piezoelectric materials are widely used in dynamic applications which include mechanical impact, ignition systems, vibration suppression and sensing [4]. Typical examples of piezoelectric materials include crystalline quartz, barium titanate ($BaTiO_3$), vanadium niobate and lead zirconate titanate (PZT) [3]. In recent years, research focus on lead-free piezoelectric materials has been intensified aimed at replacing lead-based materials in electronic devices for the sake of human health and preservation of the natural environment [5].

Piezoelectric materials are produced as multilayered components consisting of electrode-ceramic stacks which can be simple/complex shapes. Various techniques have been developed to fabricate the piezoelectric ceramics without conducting post-processing. These include injection moulding [6, 7], embossing [8] and fused deposition method [9]. The powder injection moulding (PIM) process has

received much attention owing to its ability to produce complex-shaped, micro-sized PZT components with minimum damage to the sintered ceramic [10]. The multilayered components are subsequently co-sintered at temperatures less than the melting point of the electrodes typically 1200–1300°C. However, lower sintering temperatures are preferred to avoid damaging the inner electrodes in the stack. It has been observed that the piezoelectric coefficient which directly influences the performance of piezoceramics is strongly influenced by the grain size [11]. Despite the extensive studies carried out over the past decades on the grain size effects on the physical properties of these materials, there are still major controversies on the dependence of piezoelectric and ferroelectric properties on the grain size [12]. There are a number of discrepancies in the existing literature which will be discussed later in this chapter.

2.2 Magnetic ceramics

Magnetic ceramic materials are extensively used in electronics and information communication fields [13]. They are generally classified as 'soft' and 'hard' magnets where soft implies large magnetic fields cannot be generated on the outside, whereas in the case of hard magnets, a magnetic field is generated around the magnet itself. Two broad groups of materials are widely used in the industry, i.e. metal magnetic materials and complex oxide containing trivalent iron ion (ferrites) magnetic materials (referred to as ceramic magnets).

Magnetic materials are generally used in the form of multilayer core of rolled thin plates or in the form of dust core [13]. At high frequencies, most metallic magnets tend to lose their magnetic properties (permeability and magnetic flux density) due to low electrical resistivity. On the other hand, ferrites (ceramic magnets) show higher electrical resistivity and smaller eddy current loss at high frequencies; hence, they are more widely used in alternating magnetic fields in comparison to metal magnetic materials. The hard ferrite is used extensively as permanent magnets for speakers and motors. One of the critical magnetic characteristics required for high-frequency materials is high permeability and is defined as the ratio between the magnetic flux density, B, and magnetic field, H, as follows:

$$\mu = \frac{B}{H} \tag{1}$$

Permeability is a structure sensitive characteristic and is strongly affected by the microstructure of the sintered material. There are two general compositions used for oxide magnetic materials, spinel type ($MeFe_2O_3$) and garnet type ($Me_3Fe_5O_{12}$); typical examples include $MnFe_2O_4$ and $Y_3Fe_5O_{12}$, respectively. Owing to the complex compositional nature of these oxides, a powder metallurgy route is normally employed for the production of oxide magnets. The microstructure and compositional control are quite critical elements of the magnetic properties of the final products. Further, magnetic properties of materials have been shown to change from those of multidomain to those of single-domain structure as the grain size is reduced below a critical size [14]. The introduction of fine-grained sintered magnetic materials has opened some opportunity for new potential applications as well as complexity on basic research [14].

2.3 Dielectric ceramics

In the last few decades, the rapid development of modern communication devices such as cellular telephones, antennas and global positioning systems has

energised research in microwave dielectric materials [15]. Dielectric ceramics are materials used widely in advanced electronic devices such as capacitors and microwave resonators. They are classified into two broad groups based on their dielectric properties. High-quality factor materials are characterised by linear changes in polarisation with applied electric field. This group is dominated by titanate-based materials which normally sinter at temperatures higher than 1100°C; typical examples include TiO_2, $MgTiO_3$, $CaTiO_3$ and $SrTiO_3$ [13]. This group is characterised by a dielectric constant ε_r of less than 1000. The second group is characterised by materials possessing a dielectric constant ε_r higher than 1000. Typical examples include $BaTiO_3$-based dielectric and lead-based dielectrics.

Ceramic capacitors are widely produced as sintered thin plates in a reducing atmosphere (low P_{O_2}). In previous studies, the particle size effects of $BaTiO_3$ on dielectric properties have been carried out with several models of the critical size of ferroelectricity being proposed. Reliability study results have shown that the dielectric layer should be pore-free with fine grain sizes (typically 0.8 μm) for enhanced performance [13].

2.4 Thermoelectric ceramics

Thermoelectric (TE) ceramic materials can directly convert heat energy to electric energy due to thermoelectric effects [16]. TEs provide an alternative environmentally friendly energy conversion technology which is compact, high reliability, has no pollutants and is feasible over a wide temperature range. The majority of thermoelectric devices operating near room temperature are based on Bismuth telluride (Bi_2Te_3) and its alloys. These materials have been produced by a variety of methods which include powder metallurgy techniques such as hot pressing (HP), SPS, Bridgman and zone melting and high-pressure sintering methods. Recent studies have shown that grain refinement of Bi_2Te_3-based alloys can greatly enhance thermoelectric performance [16]. The performance of thermoelectric materials is based on a dimensionless figure of merit (ZT) as follows:

$$ZT = \frac{S^2 \delta T}{\kappa} = \frac{S^2 T}{(\kappa_e + \kappa_l)\rho} \qquad (2)$$

where S, δ, κ, ρ and T represent the Seebeck coefficient (S), electrical conductivity (δ), thermal conductivity, resistivity and absolute temperature, respectively.

Thermal conductivity of TE materials consist of two parts: lattice thermal conductivity (κ_l) and electronic thermal conductivity (κ_e). In principle, a high ZT is obtained by large values of both seeback coefficient and electrical conductivity, while thermal conductivity (κ) is minimised to maintain the temperature difference (T) producing the Seebeck coefficient [17, 18]. However, this requirement contradicts the Wiedemann-Franz law which requires the electronic part of thermal conductivity to be proportional to electrical conductivity, and the Pisarenko relation limits the simultaneous enlargement of α and δ [19]. This makes it difficult to enhance the ZT using the tuning of carrier concentration alone.

Over the years, a number of strategies have been adopted to enhance the power factor and reduce thermal conductivity of TEs. This has resulted in the development of three generations of TEs over the 200-year period since their discovery in 1821. The development history has been characterised by achieving high ZTs > 2.0 through new concepts and technologies. The first TE generation devices are characterised by ZT ~ 1.0 operating at power conversion efficiencies of 4–5% [17]. In the 1990s the introduction of nanostructures increased the ZT values by about 70% to ZT ~ 1.7, and the power conversion efficiencies can be expected to be 11–15%. In the

third generion, some new concepts such as band structure engineering by doping, reduction in lattice thermal conductivity, nanostructuring and all-scale hierarchical architecturing and quantum confinement effects have been introduced to enhance Seebeck coefficients [16].

3. Processing of functional ceramic materials

It is apparent that the increasing demand for ceramic materials in more advanced technological applications has resulted in greater need for improved properties and reliability of functional materials [2, 13]. The fabrication process plays a critical role in final material characteristics. In other words, the properties of ceramic materials are dictated by the microstructure which is a function of the processing method utilised. Thus microstructures can be tailored through fabrication processes to produce desired properties. In the past few decades, there has been a wide acceptance among powder metallurgists that the quality and reliability of ceramic materials are largely dictated by utilising powders of controlled purity, particle size and size distribution, shape and degree of agglomeration. The characteristics of starting powders are determined by their production method of which a variety of methods are available for the production of ceramic materials. The processing methods are broadly classified into solid-state processing (e.g. mechanical alloying, self-propagating high-temperature synthesis (SHS), laser ablation) and solution chemistry (e.g. sol-gel, polymer pyrolysis, hydrothermal methods) [2]. The chemical processing methods are generally more expensive than solid-state methods but offer more strict control of the powder characteristic [13]. The choice of a powder processing route will therefore largely depend on the production cost and its capability to achieve desired powder characteristics.

Chemical methods involving chemical reactions under carefully controlled conditions normally result in ultrafine nanometric powders (<100 nm) with a narrow particle size distribution [13]. The main attraction in using nanometric powders is their ability to sinter at lower temperatures (typically <0.5 Tm); this is in accordance with Hering's law discussed in the next section. The diffusion distance during sintering is drastically shortened in nanostructured powders. Moreover, an enhancement of material properties is expected owing to a reduction in the flaw size, and a higher density of highly disordered interfaces is also attained at nanometric particle size range. On the other hand, powders produced by mechanical methods possess a wide particle size distribution which may lead to higher packing density in the green body. However, this advantage is far outweighed by the difficulty in microstructural control during sintering as large grains grow uncontrollably at the expense of the smaller grains, thus making grain size control impossible. However, it is important to underline that as particle size decreases, below ~0.5 μm, particles become more difficult to handle and tend to agglomerate resulting in nonuniform consolidation of powders. Thus the use of nanopowders requires proper control and handling to ensure high-quality properties are attained in the final products.

4. Spark plasma sintering technology

In 1906, Bloxam filed the first patent on the successful consolidation of powder using the SPS technology [20]. Steady progress was made in the mid-1980s into the 1990s. The SPS technology sinters in a conducting die with a simultaneously applied mechanical pressure and DC pulses which allows for simultaneous densification

and sintering process [21]. The SPS set-up consists of a graphite die filled with powder feedstock, uniaxial hydraulic pressing device which achieves 50–250 kN and an electric pulse current of low voltage (<10V) and high currents (1–10 kA) [2]. The system has achieved heating rates of up to 1000°C/min which makes it possible to sinter over very short durations [22]. It can be operated under vacuum or inert gas atmosphere at atmospheric pressure with a maximum temperature of 2400°C.

The sintering mechanisms in SPS are a result of three effects, namely, mechanical, thermal and electrical [2]. The fast heating rates achieved in SPS enables densification while retarding microstructure coarsening owing to the short times required to reach sintering temperature. This allows for the densification of nanopowders with minimal grain coarsening [22]. The SPS system offers a number of advantages over the conventional sintering systems such as hot pressing, hot isostatic pressing (HIP) which include high sintering speeds, high reproducibility, better control of sintering energy and reliability.

The mechanism of sintering is not well understood but several authors have postulated a number of theories. The widely accepted SPS sintering mechanisms involve joule heating, plasma generation and electroplastic effect [2]. The electrical effects are a function of the electrical properties of the powders. For powders that are electrically conducting, current can easily flow through, and heat is generated mainly by joule heating and transferred to the bulk of the powder by conduction (see **Figure 1**) [23]. In the presence of an applied pressure, the electric current through the particles enhances formation of interparticle bonds through localised welding, vaporisation or cleaning of powder surfaces [22]. This ensures a smoother and more favourable path for the current flow. This also promotes the production of high-quality sintered compacts at lower temperatures in a shorter time than conventional sintering methods. The sintering of nonconducting powders, although not well understood, is thought to occur through grain boundary migration and matter transport at higher input voltages.

Although the SPS has the capability to sinter at high heating and cooling rates, the expectation is that the system can sinter without appreciable grain growth. However in reality this is not always the case; a complete avoidance of the grain growth at the sintering temperatures for most nano-grained materials will always promote grain growth. It is therefore imperative to adopt an approach/methodology
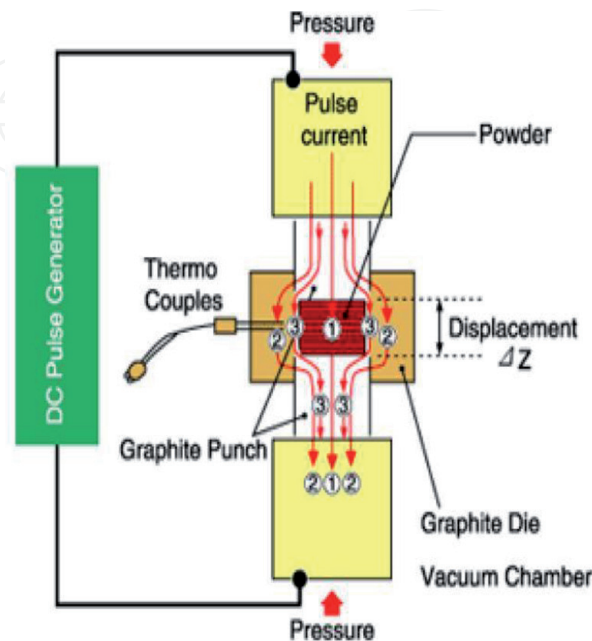

Figure 1.
Pulse current flow through the spark plasma sintering technology [22].

that is more effective in minimising grain growth using the SPS system. The *two-step* sintering (TSS) approach has been found to be effective in minimising grain growth of ceramic materials during sintering. It is thus important to dedicate the following section to the success studies on the sintering of functional ceramics to give an insight and a better understanding of the TSS method.

5. Two-step sintering methodology

The reliability of ceramic materials is a key function, and it dictates their ultimate performance. A carefully controlled microstructure has a greater impact on the properties and reliability of functional ceramic materials. In the previous section, it has been shown that the development of highly dense nanometric or ultrafine-grain-sized ceramics is not easily achievable through conventional sintering. Although the SPS technology has shown great potential in the production of highly dense nano-metric materials, it is difficult to maintain microstructural refinement under the high sintering temperatures. It must be underlined that solid-phase sintering requires high temperatures to facilitate diffusion which promotes material densification. However diffusion processes promote not only densification but also grain growth [24]. To achieve grain refinement during sintering, it is therefore imperative to develop a sintering methodology which promotes only densification without stimulating grain growth. This method has been improved over the years to achieve better microstructural refinement. The so-called two-step sintering (TSS) was subsequently intro-duced in the 1990s by Chu et al. [25]. In essence, the technique consists of two stages of consolidation process, i.e. a first stage performed at relatively low temperature followed by a higher-temperature stage and subsequent cooling.

However, the higher-temperature stage if not adequately controlled can lead to some grain growth. In 2000, Chen and Wang proposed a modified TSS methodol-ogy which effectively suppresses the accelerated grain growth in the second stage [24, 26]. In the modified TSS approach, a high-temperature heating is performed first for a short duration followed by structural freezing and sintering at a lower temperature. The idea of heating to a higher temperature (T1) followed by fast cooling with no sintering holding time (stage 1 in **Figure 2**) is to eliminate residual porosity at higher temperature and develop a network of grain boundary anchoring at triple points [11].

These anchored triple points are thought to have higher activation energy for matter migration than the grain boundaries. The second step effectively proceeds in
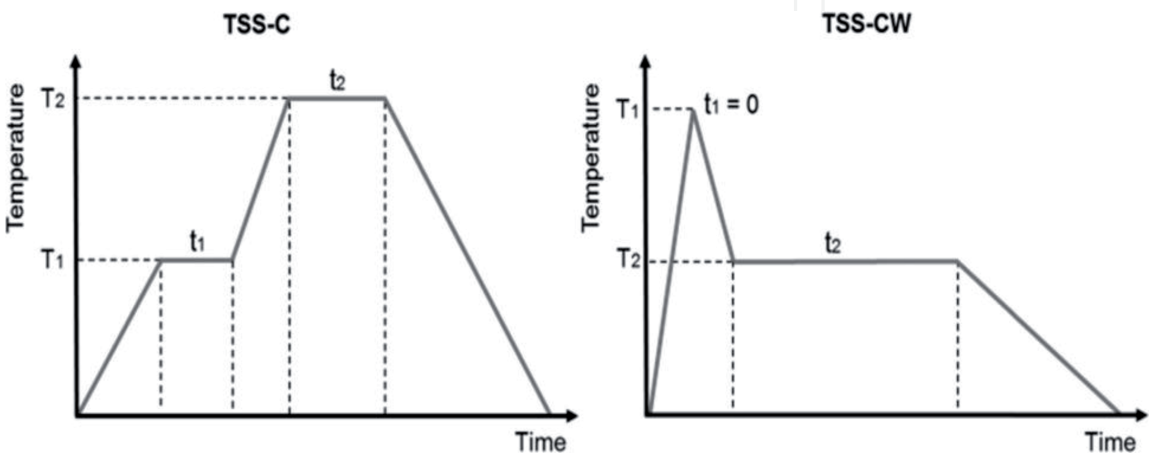

Figure 2.
Schematic illustration of the differences between the two TSS approaches [11].

a *frozen* microstructure due to slower kinetics [27, 28]. The *kinetic window* separates grain boundary diffusion and grain boundary migration. Grain growth experienced at intermediate and high temperatures in fine-grained materials is driven by the significantly higher capillary pressures available in ultrafine grains. For instance, for a grain boundary energy (and surface energy) in ceramics of 1 J/m^2, a capillary pressure of the order 20 MPa at 100 nm, 200 MPa at 10 nm and 2000 MPa at 1 nm grain size. This implies there are significantly higher pressures locked in ultrafine grains to ignite additional kinetic effects at elevated temperatures. Thermodynamically, the temperature (T2) is sufficiently high to allow grain boundary diffusion with minimal grain boundary migration; this promotes densification without significant grain growth. It is however important to select the most suitable T2 temperature. In the case that T2 is too low, sintering proceeds for a prolonged period until it becomes exhausted; on the other hand, if T2 is too high, grain growth is likely to occur.

5.1 Two-step sintering as applied to functional ceramic materials

The use of the TSS methodology to obtain ceramic materials of controlled microstructure has become standard practice. This section gives a detailed discussion on the effects of processing characteristics on grain density and size as well as their contribution to the improvement of mechanical properties of a number of functional ceramic materials investigated in previous studies.

The pioneering work of Cheng and Wang in 2000 serves as the beginning of a new era in TSS methodology. In one of their successful studies, Chen and Wang obtained a density of 99% and a grain size of 123 nm using a T1 temperature of 1250°C and T2 temperature of 1100°C for a pure Y$_2$O$_3$ ceramic material [24, 26]. After several experimental studies, Chen and Wang concluded that the success of grain growth suppression in their work was mainly attributed to triple-point immobility irrespective of whether doping agents were used or not [11]. In a separate study, Mazaheri et al. [29] obtained dense samples of ZnO with limited grain growth under varying conditions. The starting particle size of the ZnO was 31 nm. The most interesting result was obtained with a T1 of 800°C and T2 of 750°C; a relative density and grain size of 98% and ~68 nm were obtained, respectively [29]. The same authors proved that slightly higher temperatures (850°C and 780°C for T1 and T2, respectively) resulted in grain growth and a lower densification of 86% using ZnO material [29]. A further study done at even higher temperatures, with a starting ZnO powder of grain size of 400 nm (0.4 μm) and a T1 of 1100°C and T2 of 1050°C, resulted in a relative density of 95.1% and a grain size of 3.9 μm, signifying the ineffectiveness of the TSS methodology at higher sintering temperatures and larger particle sizes. Several other TSS studies carried out on the ZnO material proved that the use of dopant agents such as Bi$_2$O$_3$, Sb$_2$O$_3$, CoO and MnO assisted in suppressing grain growth [11].

Yttria-stabilised ZrO$_2$ (YSZ) is one of the most important functional ceramics which find its use in a wide range of applications. Several attempts have been focused on attaining nanometric YSZ materials to improve its functional properties. Mazaheri et al. [30] obtained fully densified 3YSZ with an initial grain size of 75 nm and a pressureless sintering regime of T2 (1150°C) and T1 (1300°C) with an isothermal holding time of 30 h at T2 and 1 min holding time at T1. The final grain size achieved was 110 nm. In a separate study, Suarez compared SPS sintering with pressureless TSS methodologies. The starting material was a three Y$_2$O$_3$-stabilised tetragonal ZrO$_2$ (3YTZ) with an initial average particle size of 65 nm. The TSS methodology used a pressureless sintering regime as T1 at 1350°C without holding time and T2 at 1200°C for 15 h, and a final grain size of 125 nm was obtained. On the other hand, the SPS method was carried out at 1150°C with a heating rate of 300°C/min and an isothermal holding time of 30 mins at a pressure of 150 MPa.

The grain size obtained was 115 nm. Several other modifications as summarised in **Table 1** were carried out, and an observation that was common to the majority of the studies is that the homogeneity of the green body was very critical to the success of the sintering method in its effectiveness of grain growth control [11].

As mentioned earlier, piezoelectric materials' performance is strongly influenced by the grain size of the constituent particles making up the ceramics. High-performing piezoceramics have been obtained using the TSS approach. A number of studies have shown that lower sintering temperatures using the TSS methodology can be utilised to obtain ultrafine grain sizes. $BaTiO_3$ is one of the most popular piezoceramics studied, and a number of studies have been carried out to obtain fine-grained microstructures. In their work, Kim and Han [31] used a 1% dysprosium (Dy)-doped $BaTiO_3$ with a particle size of approximately 17 nm which was compacted at 300 MPa at room temperature. The TSS profile used a T1 of 1300°C and a T2 of 1100°C with a 20 h holding time. A grain size close to 1 µm was obtained at a relative density of 95%. In a separate study, Wang et al. [32] studied two different piezoceramic composites, i.e. pure $BaTiO_3$ with a particle size between 10 nm and 30 nm and a nanometric ferrite of composition $Ni_{0.2}Cu_{0.2}Zn_{0.6}Fe_2O_4$ with a starting particle size of 10 nm. The two powders were compacted isostatically at 200 MPa. The two piezoceramics were sintered using two different sintering programmes, i.e. a T1 of 950–1250°C for $BaTiO_3$ and at 850–930°C for ferrite; a cooling rate of 10°C/min was used in both cases. The samples were cooled at 30°C/min to a

Sample	Method	Starting grain size (nm)	Pressure (MPa)	T1 profile (°C)	T2 profile (°C)	Relative density (%)	Grain size	Ref
Pure Y_2O_3	TSS	10–60	—	10°C/min to 1250	50°C/min to 1100, 6–30 h dwell	99	123 nm	[24, 26]
Pure ZnO	TSS	31	—	800	750	98	680 nm	[29]
Pure ZnO	TSS	400	—	1100	1050	95.1	3.9 µm	[34]
3YSZ*	TSS	0.27 µm	—	1500 (5 min) 10°C/min	1300, 10 h	—	0.59 µm	[35]
3YSZ	TSS	75	150	1300, 1 min	1150, 30 h	Density at T1 (83)	110 nm	[30]
3YSZ	SPS	65	150	—	1150, 150 MPa, 300°C/min, 30 min	—	115 nm	[36]
3YSZ	TSS	65	—	1300	1200, 15 h	—	—	[36]
3YSZ	TSS	60–120	—	1300, 10°C/m	1175, 20 h	99.2	184 nm	[37]
3YSZ	H-SPS	60–120	100 at 600°C, 3 min	300 MPa at 1000, 5 min	1175, 300 MPa, 30 h	97.4	173 nm	[37]
8YSZ	SPS	58	50, 15 min	1150, 200 °C/min, 20 s, 10 MPa	1050, 50 MPa, 2 h	99.8	190 nm	[38]

*3YSZ, 3 mol% Y_2O_3-stabilised ZrO_2.

Table 1.
A summary of the two-step methodology used to produce different materials.

T2 range of 1150–850°C for BaTiO$_3$ and 750–870°C for the ferrite with an isothermal holding time of 20 h. For the BaTiO$_3$, the best result achieved showed a grain size of 35 nm and was sintered at 950°C in T1 and at 900°C in T2 for 2 h. On the other hand, a grain size of 200 nm was achieved for the ferrite sintered at 850°C in T1 and 800°C for 6 h in T2. In comparison to the result of Kim and Han discussed earlier, the use of a lower sintering temperature enabled the formation of BaTiO$_3$ with a finer grain size. To elucidate this point, Karaki et al. [33] obtained a mean grain size of 1.6 μm with a relative density of 98.3% starting with a BaTiO$_3$ of average particle size of 100 nm, cold compacted at 200 MPa. A TSS profile almost similar to that of Kim and Han et al. consists of a heating rate of 10°C/min to T1 (1230–1340°C) held for 1 min and a cooling rate of 30°C/min to T2 (1150–1200°C) held for 2, 4, 5 and 20 h. The best result was obtained with a sintering profile consisting of T1 (1320°C) and T2 (1150°C) with a 15 h holding time. There is a clear indication from the above results that BaTiO$_3$ ceramics with high sintered density are obtainable at lower sintering temperature (≤1000°C) for both T1 and T2. Some of the authors observed that the piezoelectric coefficient is strongly influenced by the grain size [11]. Nanometric BaTiO$_3$ ceramics possess superior piezoelectric coefficients in comparison to their micrometric counterparts.

As mentioned earlier, the current work is not meant to be exhaustive but to give a qualitative insight on the research covered so far. **Table 1** gives a summary of some of the successful work carried out and highlights some critical aspects in the TSS methodology as a grain refinement process.

Specific particularities were observed in each of the sintering cycles above. The majority of the authors compared their results with those obtained by conventional sintering and the TSS methodology resulted in superior grain refinement. The initial powder features such as particle size, microstructural homogeneity and green density are quite critical in the success of the TSS process. In the majority of cases, the difference between the T1 and T2 temperatures is <1500°C, and a larger holding time in T2 allowed smaller grain sizes to be obtained. The TSS method has also been shown to improve the material properties (both mechanical and physical).

In some cases the use of dopants was effective in inhibiting grain growth. Although the TSS approach has shown great success in effecting grain refinement, the very long isothermal holding times at T2 might not be suitable for commercial purposes. The SPS technology offers an alternative route for grain refinement, and results in **Table 1** show that it is more effective for materials such as YSZ ceramics. The SPS process generally can achieve grain refinement over shorter time periods.

6. The use of SPS technology in the synthesis of functional ceramic materials

SPS technology provides an alternative and more effective route for grain refinement of ceramic materials. As discussed earlier, conventional sintering is ineffective in refinement of ceramic materials owing to the excessive grain growth of fine powders at elevated temperatures [20–22]. The TSS methodology was developed to mitigate this problem, and it provides a low-cost and effective route for grain refinement. However, this method requires very long isothermal holding times to effect sintering without grain growth. Therefore, it might not be suitable for high production rates (commercial purposes); in addition the prolonged holding times are likely to increase the energy costs. Moreover, there are ceramics that require pressure-assisted sintering to impart the required strength to the component during sintering. The shortcomings above can be minimised with the use of SPS technology which has been briefly discussed in the previous section.

The SPS technology has been successfully used in the production of nanometric functional ceramic materials. The discussion below presents some examples where SPS has been utilised to obtain bulk ceramic nanomaterials. The discussion is not meant to be exhaustive but to impart some critical in-depth knowledge on the synthesis procedures of a few selected case studies.

6.1 SPS of nanostructured magnetic ceramics

The magnetic properties of ferrites (magnetic ceramics) are structure sensitive and are affected by a number of factors such as phase composition, crystallite size and shape and the quantity of heterogeneities [39]. It is therefore critical to use a synthesis method capable of producing superior magnetic properties through control of structural homogeneities. The use of SPS technology is thought to promote ordering of spatial positions of magnetic moments of metal ions in the composite crystal lattice through pressure-assisted sintering [40]. The result is the formation of new magnetic phases through a pressure-induced transformation of the nanocrystalline phases [39]. It must be noted however that the mechanism of this transformation in SPS is not well developed for most of the ceramic ferrites.

Papynov and co-workers studied the magnetic properties of nanostructured ferrites using SPS technology (α-Fe_2O_3 and α-Fe_2O_3-Fe_3O_4 composite) [39]. The authors established that the value of magnetisation increases significantly with increasing sintering temperature and reached a value of 10.2 emu/g at 1100°C (equivalent to a tenfold increase). This was attributed to changes in the crystalline phase and to a lesser extent growth of ferrite grains which may affect magnetisation.

In their work Gaudisson et al. [41] consolidated a nanosized magnetic powder into a high-density solid at 750°C for 15 min to a final grain size range of 150 nm. In a separate study, a nanostructured Co-ferrite was shown to be sensitive to heating rate under the same sintering temperatures and times in SPS. A higher heating rate (80°C/min) maintained a finer grain size of 70 nm than a lower heating rate (15°C/min) which produced a grain size of 290 nm for two powders which were processed at the same sintering temperatures and times (2 min at 600°C followed by 5 min at 500°C) [41]. Ultrafine, highly dense yttrium iron garnet (YIG) was produced by SPS treatment at 750°C for 15 min at 100 MPa in wide contrast to the typical parameters used in conventional sintering which requires higher sintering times (typically 1350°C for a few hours) [42].

A $SrFe_{12}O_{19}$ hexaferrite with a grain size of 400 nm was obtained using SPS at 1100°C for 5 min with a maximum density of 5.15 g/cm³. There was a big contrast with conventional sintering at 1240°C for 2 h which produced a density of 4.83 g/cm³ and a grain size double that of the SPS-produced material [43]. Harder magnetic properties were obtained from the SPS-produced ferrite. In another study, harder magnetic properties were obtained for an SPS-sintered Ba-hexaferrite owing to limited grain growth; grains of 100–150 nm were obtained in comparison to conventional sintering which produced a grain size of 1.5–8 μm [44].

6.2 SPS of nanostructured piezoceramics

The grain size effect on the macroscopic functional properties of piezoceramics has been widely researched. There are however very few studies that correlate grain size and property stability. It has been shown that improved performance, high permittivity miniaturised devices can be obtained by microstructural control such as grain size and homogeneity [45]. Arlt and co-workers have shown the strong dependency of $BaTiO_3$ functional properties on the microstructure and grain size [46]. Moreover, large grain sizes are detrimental to the mechanical strength of ceramic-based devices.

Several studies have been dedicated towards investigating the effect of grain size on the piezoelectric properties of $BaTiO_3$ ceramics down to nanometric scale.

$BaTiO_3$-based piezoceramics is one of the most studied using SPS. It has been demonstrated that SPS technology is effective in stabilising the metastable $BaTiO_3$ cubic phase and reducing the intergranular effects on permittivity and DC resistance [45]. Moreover, SPS samples have shown higher permittivity values typically below the Curie temperature (Tc) [47]. It has been demonstrated that at finer grain sizes, the dielectric constant at the transition temperature decreases and Tc shifts to lower temperatures [45].

Lead-based piezoceramics have dominated the market of piezoelectric ceramics for a long time. However, their continued use is now questionable owing to the associated health risk especially during processing. Another major concern in the sintering of PZT piezoceramics ($Pb(Zr,Ti)O_3$) is the high sintering temperatures which promote the vitalization of lead [48, 49]. Moreover, a number of the proposed alternative piezoceramic materials also contain highly volatile elements such as in $(Na,K)NbO_3$ which makes their sintering ability quite poor. The use of SPS has enabled suppression of lead loss through rapid heating rate, lower sintering temperature and shorter sintering times [50]. In one study, Han et al. demonstrated that the use of SPS can lower the sintering temperature of a $Pb (Zr_{0.52}Ti_{0.42}Sn_{0.02}Nb_{0.04})O_3$ piezoceramic by a substantial 200–300°C while maintaining a high relative density (>99%) [51]. In a separate study, a $(Na_{0.535}K_{0.485})_{1-x}Li_x(Nb_{0.8}Ta_{0.2})O_3$ (x = 0.02–0.07) ceramic with improved mechanical and electrical properties was produced using SPS method [52].

There is an assumption that the nonlinear response of piezoceramics is grain size dependent; this is understood to be the variation of functional properties under an external stimulus. The two major contributors to nonlinear response of piezoceramics are the intrinsic (i.e. the contribution of composition, crystal structure, etc.) and extrinsic (i.e. grain size, domain wall dynamics, etc.) contributors [53, 54]. This implies that a significant decrease in grain size has the potential to produce a notable modification of nonlinear response in piezoceramics. It therefore means the stability of piezoelectric properties may be improved by controlling the grain size.

6.3 SPS of nanostructured thermoelectric ceramics

The wide application of TEs has not been realised mainly owing to low conversion efficiencies. For instance, commercially available TE materials possess a low ZT of 1 and average conversion efficiency of ~5% [55]. In order to promote the practical applications of TEs, it is critical to synthesise TE materials with ZT values >1; a TE device with ZT = 3 operating between room temperature and 773 K would yield ~ 50% of the Carnot efficiency [56]. It is evident from previous reviews that the key strategy in the improvement of ZT values for TEs has been the increase in the seeback coefficient and reduction in thermal conductivity. However, no significant improvement in ZT values has been reported through the tuning of these properties. Theoretical predictions have shown that nanostructuring can enhance the seeback coefficient through modification of density of states and can reduce the thermal conductivity by selective scattering of phonons, resulting in good ZT values. It should be noted here that the TE properties of nanostructured materials also depend on the size and morphology of microstructural features; thus, microstructural engineering is key in the development of TE materials. In 2005, Yu et al. observed that the seeback coefficient and thermal and electrical conductivities are all significantly dependent on grain size; this was confirmed on $CoSb_3$ TE materials [57].

It has been proven that the main design principle for the future TEs is the use of nanostructured architectures. A number of approaches have been utilised in

developing nano-inclusions which are effective in reducing the lattice thermal conductivities [16]. Such methods include in situ dispersion of partially oxidised nanoparticles in matrix [58], endotaxial nanoprecipitates [59, 60] and embedded nano-inclusions [61, 62]. The SPS technology has been utilised in fabricating highly dense and fine-grained TEs [63]. Nanocomposite grains are believed to be effective in scattering phonons with a broad wavelength which enhances the functional properties of TEs [55]. By nanostructuring a wide variation in ZT values ranging from 0.4 to 1.7 has been obtained for nanocomposites with similar composition. A ZT of about 1.5 at 390 K was achieved for a $(Bi,Sb)_2Te_3$ nanocomposite produced by a combination of melt spinning of single elements followed by SPS sintering. Another $Bi_{0.52}Sb_{1.48}Te_3$ nanocomposite material had a ZT ~ 1.56 [64, 65]. It has also been proven that by combining mechanical alloying and SPS sintering, one can achieve high ZT of 1.5 at 700 K in $AgPbmSbTe_{m+2}$ nanocomposite [66].

Most of the bulk TE materials with highest ZT values are fabricated through the SPS process. Bi_2Te_3 compounds have been produced with ZT values ranging from 0.7 to 1.8 in the SPS [67]. The reason for a wide range of ZT values has been attributed to varying initial green densities which is key in determining the inner temperature of the sample. Moreover, powder aggregates can lead to inhomogeneous distribution of temperature.

7. Conclusion

There is clear evidence that SPS technology and TSS methodology have yielded quite some progressive results in the production of functional nanoceramic materials. Moreover, the use of modified TSS methodology in SPS equipment has shown great potential for yielding nanostructured materials with minimum risk of grain growth. However, what still remains controversial is the consistency of the functional properties and reproducibility of the methodologies used. Thus this area of study still remains highly energised for a broader enquiry. Furthermore, for most functional ceramic materials, nanostructuring has yielded enhanced material properties through various mechanisms. Although there is still room for improvement, it remains a challenge to material scientists and engineers alike to explore further and develop a deeper understanding of the mechanisms involved which may help achieve large increases in critical functional properties. Some of the highlighted problems which might have contributed to the inconsistences in functional properties include variations in the starting green densities and the likelihood of powder agglomeration at these finer sizes. This leads to inhomogeneous temperature distribution in samples and variations in sintered densities which has direct impact on material properties.

In conclusion, for practical purposes most of these materials have to satisfy certain conditions for this to become a reality: the synthesis route should be scalable, high quality and low cost, materials should have the ability to form dense compact nanostructured materials which are amenable to subsequent processing such as machining/device integration and lastly the nanostructured products should demonstrate enhanced functional properties over their micron-sized counterparts. This points to exciting scientific opportunities for continued research in order to gain more quantitative understanding to allow the design and optimisation of processes in the development of functional ceramic materials.

Author details

Wallace R. Matizamhuka
Department of Metallurgical Engineering, Vaal University of Technology,
Vanderbijlpark, South Africa

*Address all correspondence to: wallace@vut.ac.za

IntechOpen

References

[1] Anselmi-Tamburini U, Spinolo G, Maglia F, Tredici I, Holland TB, Mukherjee AK. Field assisted sintering mechanisms. In: Sintering. Berlin, Heidelberg: Springer; 2012. pp. 159-193. DOI: 10.1007/978-3-642-31009-6_8

[2] Matizamhuka WR. Spark plasma sintering (SPS)-an advanced sintering technique for structural nanocomposite materials. Journal of the Southern African Institute of Mining and Metallurgy. 2016;**116**(12):1171-1180. DOI: 10.17159/2411-9717/2016/v116n12a12

[3] Riedel R, Ionescu E, Chen I-W. Modern trends in advanced ceramics. Ceramics Science and Technology. Weinheim, Germany: Wiley-VCH; 2008. 3-38 p. ISBN: 978-3-527-31155-2

[4] Patel I. Ceramic Based Intelligent Piezoelectric Energy Harvesting Device. London, UK: INTECH Open Access; 2011. DOI: 10.5772/19189

[5] Uchino K. The development of piezoelectric materials and the new perspective. In: Advanced Piezoelectric Material. Sawstone, Cambridge, UK: Woodhead Publishing; 2017. pp. 1-92. DOI: 10.1016/B978-0-08-102135-4.00001-1

[6] Bowen LJ, French KW. Fabrication of piezoelectric ceramic/polymer composites by injection molding. In: ISAF'92: Proceedings of the Eighth IEEE International Symposium on Applications of Ferroelectrics. Greenvile, SC, USA: IEEE; 1992. pp. 160-163. DOI: 10.1109/ISAF.1992.300651

[7] Shin HY, Kim JH, Jang JS, Baek SM. FEA for fabrication process of PZT preform using cim. Journal of the Korean Ceramic Society. 2009;**46**(6):700-707. DOI: 10.4191/KCERS.2009.46.6.700

[8] Su B, Zhang D, Button TW. Embossing of ceramic micro-pillar arrays. Journal of the European Ceramic Society. 2012;**32**(12):3345-3349. DOI: 10.1016/j.jeurceramsoc.2012.04.009

[9] Bandyopadhyay A, Panda RK, Janas VF, Agarwala MK, Danforth SC, Safari A. Processing of piezocomposites by fused deposition technique. Journal of the American Ceramic Society. 1997;**80**(6):1366-1372. DOI: 10.1109/ISAF.1996.598197

[10] Han JS, Gal CW, Kim JH, Park SJ. Fabrication of high-aspect-ratio micro piezoelectric array by powder injection molding. Ceramics International. 2016;**42**(8):9475-9481. DOI: 10.1016/j.ceramint.2016.03.011

[11] Lóh NJ, Simão L, Faller CA, De Noni A Jr, Montedo ORK. A review of two-step sintering for ceramics. Ceramics International. 2016;**42**(11):12556-12572. DOI: 10.1016/j.ceramint.2016.05.065

[12] Tan Y, Zhang J, Wu Y, Wang C, Koval V, Shi B, et al. Unfolding grain size effects in barium titanate ferroelectric ceramics. Scientific Reports. 2015;**5**:9953. DOI: 10.1038/srep09953

[13] Somiya S. Handbook of Advanced Ceramics: Materials, Applications, Processing, and Properties. Waltam, USA: Academic Press; 2013. ISBN: 978-0-12-385469-8

[14] Breitwieser R, Acevedo U, Ammar S, Valenzuela R. Ferrite nanostructures consolidated by spark plasma sintering (SPS). In: Nanostructured Materials-Fabrication to Applications. Janeza, Croatia: IntechOpen; 2017. DOI: 10.5772/68017

[15] Filipović S, Pavlović VP, Obradović N, Paunović V, Maca K, Pavlović VB. The impedance analysis of sintered $MgTiO_3$ ceramics. Journal of Alloys and

Compounds. 2017;**701**:107-115. DOI: 10.1016/j.jallcom.2017.01.117

[16] Zhang X, Zhao LD. Thermoelectric materials: Energy conversion between heat and electricity. Journal of Materiomics. 2015;**1**(2):92-105. DOI: 10.10 16/j.jmat.2015.01.001

[17] Zhao LD, Dravid VP, Kanatzidis MG. The panoscopic approach to high performance thermoelectrics. Energy & Environmental Science. 2014;**7**(1): 251-268. DOI: 10.1039/C3EE43099E

[18] He J, Kanatzidis MG, Dravid VP. High performance bulk thermoelectrics via a panoscopic approach. Materials Today. 2013;**16**(5):166-176. DOI: 10.1016/j. mattod.2013.05.004

[19] Dresselhaus M. Overview of thermoelectrics for thermal to electrical energy conversion. AIP Conference Proceedings. 2013;**1519**(1):36-39. DOI: 10.1063/1.4794704

[20] Bloxam AG. Improved manufacture of electric incandescence lamp filaments from tungsten or molybdenum or an alloy thereof. GB Patent. 1906;**27**:13

[21] Tokita M. Recent and future progress on advanced ceramics sintering by Spark Plasma Sintering. Nanotechnologies in Russia. 2015;**10**(3-4):261-267. DOI: 10.1134/S1995078015020202

[22] Suarez M, Fernandez A, Menendez JL, Torrecillas R, Kessel HU, Hennicke J, et al. Challenges and opportunities for spark plasma sintering: A key technology for a new generation of materials. In: Ertu B, editor. Sintering Applications. Janeza, Croatia: InTech; 2013. pp. 319-342. DOI: 10.5772/53706. Ch. 13

[23] Guillon O, Gonzalez-Julian J, Dargatz B, Kessel T, Schierning G, Räthel J, et al. Field-assisted sintering technology/spark plasma sintering: Mechanisms, materials, and technology developments. Advanced Engineering Materials. 2014;**16**:830-848. DOI: https://doi.org/10.1002/adem.201300409

[24] Chen IW, Wang XH. Sintering dense nanocrystalline ceramics without final-stage grain growth. Nature. 2000;**404**(6774):168, 35004548

[25] Chu MY, De Jonghe LC, Lin MK, Lin FJ. Precoarsening to improve microstructure and sintering of powder compacts. Journal of the American Ceramic Society. 1991;**74**(11):2902-2911. DOI: 10.1111/j.1151-2916.1991.tb06861

[26] Wang XH, Chen PL, Chen IW. Two-step sintering of ceramics with constant grain-size, I. Y_2O_3. Journal of the American Ceramic Society. 2006;**89**(2):431-437. DOI: 10.1111/j.1551-2916.2005.00763.x

[27] Sutharsini U, Thanihaichelvan M, Singh R. Two-step sintering of ceramics. Sintering of Functional Materials. 2017:1-20. DOI: 10.5772/68083

[28] Ferreira GBP, da Silva JF Jr, do Nascimento RM, Gomes UU, Martinelli AE. Two-step sintering applied to ceramics. In: Sintering of Ceramics-New Emerging Techniques. Janeza, Croatia: InTech; 2012. ISBN 978-953-51-0017-1

[29] Mazaheri M, Zahedi AM, Sadrnezhaad SK. Two-step sintering of nanocrystalline ZnO compacts: Effect of temperature on densification and grain growth. Journal of the American Ceramic Society. 2008;**91**(1):56-63. DOI: 10.1111/j.1551-2916.2007.02029.x

[30] Mazaheri M, Simchi A, Golestani-Fard F. Densification and grain growth of nanocrystalline 3Y-TZP during two-step sintering. Journal of the European Ceramic Society. 2008;**28**(15):2933-2939. DOI: 10.1016/j. jeurceramsoc.2008.04.030

[31] Kim HT, Han YH. Sintering of nanocrystalline $BaTiO_3$. Ceramics International. 2004;**30**(7):1719-1723. DOI: 10.1016/j.ceramint.2003.12.141

[32] Wang JC, Zheng P, Yin RQ, Zheng LM, Du J, Zheng L, et al. Different piezoelectric grain size effects in $BaTiO_3$ ceramics. Ceramics International. 2015;**41**(10):14165-14171. DOI: 10.1016/j.ceramint.2015.07.039

[33] Karaki T, Yan K, Adachi M. Barium titanate piezoelectric ceramics manufactured by two-step sintering. Japanese Journal of Applied Physics. 2007;**46**(10S):7035. DOI: 10.1143/JJAP.46.7035/meta

[34] Wu MW. Two-step sintering of aluminum-doped zinc oxide sputtering target by using a submicrometer zinc oxide powder. Ceramics International. 2012;**38**(8):6229-6234. DOI: 10.1016/j.ceramint.2012.04.076

[35] Mazaheri M, Zahedi AM, Haghighatzadeh M, Sadrnezhaad SK. Sintering of titania nanoceramic: Densification and grain growth. Ceramics International. 2009;**35**(2):685-691. DOI: 10.1016/j.ceramint.2008.02.005

[36] Suárez G, Sakka Y, Suzuki TS, Uchikoshi T, Zhu X, Aglietti EF. Effect of starting powders on the sintering of nanostructured ZrO_2 ceramics by colloidal processing. Science and Technology of Advanced Materials. 2009;**10**(2):025004. DOI: 10.1088/1468-6996/10/2/025004

[37] Xiong Y, Hu J, Shen Z. Dynamic pore coalescence in nanoceramic consolidated by two-step sintering procedure. Journal of the European Ceramic Society. 2013;**33**(11):2087-2092. DOI: 10.1016/j.jeurceramsoc.2013.03.015

[38] Schwarz S, Guillon O. Two step sintering of cubic yttria stabilized zirconia using field assisted sintering technique/spark plasma sintering. Journal of the European Ceramic Society. 2013;**33**(4):637-641. DOI: 10.1016/j.jeurceramsoc.2012.10.002

[39] Papynov EK, Tkachenko IAE, Portnyagin AS, Modin EB, Avramenko VA. Fabrication of magnetic ceramic materials based on nanostructured hematite powder by spark plasma sintering. Carbon (C). 2006;**4**(243):2-5. ISSN 1819-6608

[40] Saravanan P, Hsu JH, Sivaprahasam D, Kamat SV. Structural and magnetic properties of γ-Fe_2O_3 nanostructured compacts processed by spark plasma sintering. Journal of Magnetism and Magnetic Materials. 2013;**346**:175-177. DOI: 10.1016/j.jmmm.2013.07.023

[41] Gaudisson T, Vázquez-Victorio G, Bañobre-López M, Nowak S, Rivas J, Ammar S, et al. The Verwey transition in nanostructured magnetite produced by a combination of chimie douce and spark plasma sintering. Journal of Applied Physics. 2014;**115**(17):17E117. DOI: 10.1063/1.4863164

[42] Gaudisson T, Acevedo U, Nowak S, Yaacoub N, Greneche JM, Ammar S, et al. Combining soft chemistry and spark plasma sintering to produce highly dense and finely grained soft ferrimagnetic $Y_3Fe_5O_{12}$ (YIG) ceramics. Journal of the American Ceramic Society. 2013;**96**(10):3094-3099. DOI: 10.1111/jace.12452

[43] Boda SK, Thrivikraman G, Panigrahy B, Sarma DD, Basu B. Competing roles of substrate composition, microstructure, and sustained strontium release in directing osteogenic differentiation of hMSCs. ACS Applied Materials & Interfaces. 2016;**9**(23):19389-19408. DOI: 10.1021/acsami.6b08694

[44] Ovtar S, Le Gallet S, Minier L, Millot N, Lisjak D. Control of barium ferrite decomposition during

spark plasma sintering: Towards nanostructured samples with anisotropic magnetic properties. Journal of the European Ceramic Society. 2014;**34**(2):337-346. DOI: https://doi.org/10.1016/j.jeurceramsoc.2013.07.027

[45] Hungria T, Galy J, Castro A. Spark plasma sintering as a useful technique to the nanostructuration of piezo-ferroelectric materials. Advanced Engineering Materials. 2009;**11**(8): 615-631. DOI: https://doi.org/10.1002/adem.200900052

[46] Arlt G, Hennings D, De With G. Dielectric properties of fine-grained barium titanate ceramics. Journal of Applied Physics. 1985;**58**(4):1619-1625. DOI: 10.1063/1.336051

[47] Takeuchi T, Betourne E, Tabuchi M, Kageyama H, Kobayashi Y, Coats A, et al. Dielectric properties of spark-plasma-sintered $BaTiO_3$. Journal of Materials Science. 1999;**34**(5):917-924. DOI: 10.1016/j.msec.2016.02.027

[48] Wang K, Li JF, Zhou JJ. High normalized strain obtained in Li-modified (K, Na) NbO_3 lead-free piezoceramics. Applied Physics Express. 2011;**4**(6):061501. DOI: 10.1143/APEX.4.061501

[49] Zhang MH, Wang K, Du YJ, Dai G, Sun W, Li G, et al. High and temperature-insensitive piezoelectric strain in alkali niobate lead-free perovskite. Journal of the American Chemical Society. 2017;**139**(10): 3889-3895. DOI: 10.1021/jacs.7b00520

[50] Chen C, Liang R, Zhou Z, Zhang W, Dong X. Enhanced bipolar fatigue resistance in PMN-PZT ceramics prepared by spark plasma sintering. Ceramics International. 2018;**44**(4):3563-3570. DOI: 10.1016/j.ceramint.2017.11.051

[51] Han B, Zhao C, Zhu Z-X, Chen X, Han Y, Duan H, et al.

Temperature-insensitive piezoelectric performance in Pb ($Zr_{0.52}Ti_{0.42}Sn_{0.02}Nb_{0.04}$)$O_3$ ceramics prepared by spark plasma sintering. ACS Applied Materials & Interfaces. 2017;**9**(39):34078-34084. DOI: 10.1021/acsami.7b09825

[52] Shen ZY, Li JF, Wang K, Xu S, Jiang W, Deng Q. Electrical and mechanical properties of fine-grained Li/Ta-modified (Na, K) NbO_3-based piezoceramics prepared by spark plasma sintering. Journal of the American Ceramic Society. 2010;**93**(5):1378-1383. DOI: 10.1111/j.1551-2916.2009.03542.x

[53] Zhang QM, Wang H, Kim N, Cross LE. Direct evaluation of domain-wall and intrinsic contributions to the dielectric and piezoelectric response and their temperature dependence on lead zirconate-titanate ceramics. Journal of Applied Physics. 1994;**75**(1):454-459. DOI: 10.1063/1.355874

[54] Ochoa DA, Esteves G, Iamsasri T, Rubio-Marcos F, Fernández JF, García JE, et al. Extensive domain wall contribution to strain in a (K, Na) NbO_3-based lead-free piezoceramics quantified from high energy X-ray diffraction. Journal of the European Ceramic Society. 2016;**36**(10):2489-2494. DOI: 10.1016/j.jeurceramsoc.2016.03.022

[55] Chen ZG, Han G, Yang L, Cheng L, Zou J. Nanostructured thermoelectric materials: Current research and future challenge. Progress in Natural Science: Materials International. 2012;**22**(6): 535-549. DOI: 10.1016/j.pnsc.2012.11.011

[56] Tritt TM, Böttner H, Chen L. Thermoelectrics: Direct solar thermal energy conversion. MRS Bulletin. 2008;**33**(4):366-368. DOI: 10.1557/mrs2008.73

[57] Yu BL, Qi Q, Tang XF, Zhang QJ. Effect of grain size on thermoelectric

properties of CoSb₃ compound. Acta Physica Sinica. 2005;**54**:5763-5768

[58] Zhao XY, Shi X, Chen LD, Zhang WQ, Bai SQ, Pei YZ, et al. Synthesis of Yb_yCo_4Sb_12/Yb_2O_3 composites and their thermoelectric properties. Applied Physics Letters. 2006;**89**(9):092121. DOI: 10.1063/1.2345249

[59] Lee Y, Lo SH, Androulakis J, Wu CI, Zhao LD, Chung DY, et al. High-performance tellurium-free thermoelectrics: All-scale hierarchical structuring of p-Type PbSe–MSe Systems (M= Ca, Sr, Ba). Journal of the American Chemical Society. 2013;**135**(13):5152-5160. DOI: 10.1021/ja400069s

[60] Zhao LD, He J, Wu CI, Hogan TP, Zhou X, Uher C, et al. Thermoelectrics with earth abundant elements: High performance p-type PbS nanostructured with SrS and CaS. Journal of the American Chemical Society. 2012;**134**(18):7902-7912. DOI: 10.1021/ja301772w

[61] Zhao LD, Zhang BP, Li JF, Zhou M, Liu WS, Liu J. Thermoelectric and mechanical properties of nano-SiC-dispersed Bi₂Te₃ fabricated by mechanical alloying and spark plasma sintering. Journal of Alloys and Compounds. 2008;**455**(1-2):259-264. DOI: 10.1016/j.jallcom.2007.01.015

[62] Xiong Z, Chen X, Zhao X, Bai S, Huang X, Chen L. Effects of nano-TiO₂ dispersion on the thermoelectric properties of filled-skutterudite Ba_0.22Co_4Sb_12. Solid State Sciences. 2009;**11**(9):1612-1616. DOI: 10.1016/j.solidstatesciences.2009.06.007

[63] Noguchi T. Powder processing of thermoelectric materials-focusing on SiGe with new sintering technique. In: XVI ICT'97. Proceedings ICT'97. 16th International Conference on Thermoelectrics. August 1997. pp. 207-214. DOI: 10.1109/ICT.1997.667082

[64] Möchel A, Sergueev I, Wille HC, Juranyi F, Schober H, Schweika W, et al. Lattice dynamics in the thermoelectric Zintl compound Yb_14MnSb_11. Physical Review B;**84**(18):184303. DOI: 10.1103/PhysRevB; 2011.84.184303

[65] Yu C, Chen Y, Xie H, Snyder GJ, Fu C, Xu J, et al. Improved thermoelectric properties in Lu-doped Yb_14MnSb_11 Zintl compounds. Applied Physics Express. 2012;**5**(3):031801. DOI: 10.1143/APEX.5.031801

[66] Wang S, Yang J, Wu L, Wei P, Yang J, Zhang W, et al. Anisotropic multicenter bonding and high thermoelectric performance in electron-poor CdSb. Chemistry of Materials. 2015;**27**(3):1071-1081. DOI: 10.1021/cm504398d

[67] Jiang Q, Yang J, Liu Y, He H. Microstructure tailoring in nanostructured thermoelectric materials. Journal of Advanced Dielectrics. 2016;**6**(01):1630002. DOI: 10.1142/S2010135X16300024